Breast Cancer Research and Treatment (2020) 182:283–297
https://doi.org/10.1007/s10549-020-05697-0

CLINICAL TRIAL

Diffusion-weighted MRI at 3.0 T for detection of occult disease in the contralateral breast in women with newly diagnosed breast cancer

Su Min Ha[1] · Jung Min Chang[1] · Su Hyun Lee[1] · Eun Sil Kim[1] · Soo-Yeon Kim[1] · Nariya Cho[1] · Woo Kyung Moon[1]

Received: 18 March 2020 / Accepted: 18 May 2020 / Published online: 23 May 2020

Abstract

Purpose Diffusion-weighted magnetic resonance imaging (DW-MRI) offers unenhanced method to detect breast cancer without cost and safety concerns associated with dynamic contrast-enhanced (DCE) MRI. Our purpose was to evaluate the performance of DW-MRI at 3.0T in detection of clinically and mammographically occult contralateral breast cancer in patients with unilateral breast cancer.

Methods Between 2017 and 2018, 1130 patients (mean age 53.3 years; range 26–84 years) with newly diagnosed unilateral breast cancer who underwent breast MRI and had no abnormalities on clinical and mammographic examinations of contralateral breast were included. Three experienced radiologists independently reviewed DW-MRI ($b = 0$ and 1000 s/mm^2) and DCE-MRI and assigned a BI-RADS category. Using histopathology or 1-year clinical follow-up, performance measures of DW-MRI were compared with DCE-MRI.

Results A total of 21 (1.9%, 21/1130) cancers were identified (12 ductal carcinoma in situ and 9 invasive ductal carcinoma; mean invasive tumor size, 8.0 mm) in the contralateral breast. Cancer detection rate of DW-MRI was 13–15 with mean of 14 per 1000 examinations (95% confidence interval [CI] 9–23 per 1000 examinations), which was lower than that of DCE-MRI (18–19 with mean of 18 per 1000 examinations, $P = 0.01$). A lower abnormal interpretation rate (14.0% versus 17.0%, respectively, $P < 0.001$) with higher specificity (87.3% versus 84.6%, respectively, $P < 0.001$) but lower sensitivity (77.8% versus 96.8%, respectively, $P < 0.001$) was noted for DW-MRI compared to DCE-MRI.

Conclusions DW-MRI at 3.0T has the potential as a cost-effective tool for evaluation of contralateral breast in women with newly diagnosed breast cancer.

Keywords Breast cancer · MR imaging · Diffusion-weighted imaging · Dense breast · Screening

Abbreviations

ADC Apparent diffusion coefficient
DCE Dynamic contrast enhanced
DW Diffusion-weighted
DCIS Ductal carcinoma in situ

Introduction

Mammography is an established modality for early detection of breast cancer and reduction of breast cancer-related mortality and morbidity [1]. However, mammography alone has low sensitivity in women with strong family history, *BRCA* or other pathogenic mutations, personal history of breast cancer, and dense breasts [2]. Thus, various supplementary imaging modalities have been investigated for screening breast cancer and annual magnetic resonance imaging (MRI) along with mammography is recommended for women at elevated risk of breast cancer [2, 3]. Screening MRI can also be used for screening of the contralateral breast in women with newly diagnosed breast cancer and depicts occult contralateral disease in 4.1% (95% confidence interval [CI] 2.7–6.0%) of women [4, 5]. Thus far, breast MRI screening studies have mainly emphasized on the role

Electronic supplementary material The online version of this article (https://doi.org/10.1007/s10549-020-05697-0) contains supplementary material, which is available to authorized users.

✉ Jung Min Chang
imchangjm@gmail.com

[1] Department of Radiology, Seoul National University Hospital, 101 Daehak-ro, Jongno-gu, Seoul 110-744, Republic of Korea

of dynamic contrast-enhanced (DCE)-MRI [4, 6–9]. DCE-MRI is mainly performed for evaluation of disease extent and guide appropriate treatment in breast cancer patients [4, 8–11] and detects additional lesions in 6.0–34.0% compared to mammography and ultrasound [12]. However, moderate specificity of DCE-MRI also detects many benign lesions with overlapping imaging features, resulting in unnecessary biopsy and emotional distress [13]. Recent studies demonstrated that only 19.0–36.0% of MRI recommendations for biopsy yield cancer [14–16], particularly when used for preoperative evaluation of newly diagnosed breast cancer [10, 17]. In addition, there are several issues to consider with DCE-MRI, such as high cost, long scanning time, repeated use of contrast agent, and unclear cost-effectiveness for women at intermediate risk [18, 19]. There is a need to develop a safe and cost-effective supplemental imaging modality for detection of mammographically occult breast cancer.

Diffusion-weighted (DW)-MRI is a fast, unenhanced technique that measures the mobility of water molecules within tissue and provides complementary information to DCE-MRI in tumor characterization [20–22]. Breast malignancies exhibit hindered diffusion and appear hyperintense on DW-MRI with low apparent diffusion coefficient (ADC) compared to normal surrounding tissue or benign tumors [23]. In a meta-analysis of 14 studies with 1140 patients, DW-MRI alone showed pooled sensitivity and specificity of 86.0% and 75.6%, respectively, compared to 93.2% and 71.1%, respectively, for DCE-MRI alone [24]. Multiple studies including one prospective multi-center trial showed that DW-MRI can reduce unnecessary benign biopsies of suspicious mammographic or DCE-MRI-detected lesions and DW-MRI is now considered as important part of multi-parametric breast MRI protocols [25]. In addition, standardization of DW-MRI acquisition and interpretation is challenging but essential to ensure reliable sensitivity and specificity. DW-MRI can be used to detect breast cancer with higher performance at 3.0T, read-out segmented echo-planar imaging (rs-EPI), and *b* value of 1000–1500 s/mm^2 than 1.5T, basic EPI, and *b* value of 600–850 s/mm^2 [26–33]. High-resolution DW-MRI with high-field-strength allows better detection and characterization of breast lesions including subcentimeter cancers [34, 35]. Previous studies suggest DW-MRI may provide higher sensitivity than screening mammography for detection of breast malignancies [28, 32, 36]. Furthermore, in a non-blinded reader study of 118 mammographically occult lesions, 89.0% of DCE- MRI-detected malignancies were visible at DW-MRI [36]. However, there is little published literature regarding performance of DW-MRI in the consecutive women with negative findings on mammography.

Thus, the purpose of our study was to evaluate the added value of DW-MRI in the detection of clinically and mammographically occult contralateral cancer in patients with newly diagnosed breast cancer. We hypothesized that the DW-MRI of 3.0T with optimized image acquisition and standardized interpretation algorithms would improve cancer detection rate and sensitivity, even if not equal to DCE-MRI.

Materials and methods

Study cohort

This retrospective study was approved by the institutional review board, and the informed consent requirement was waived. From January 2017 through July 2018, a search of our breast imaging database revealed a total of 1885 consecutive patients with newly diagnosed unilateral breast cancer, who underwent preoperative breast MRI at 3.0T in our institution. During the study period, DW-MRI was performed as part of the standard clinical breast MRI protocol. We excluded patients who were treated with neoadjuvant chemotherapy before surgery ($n=654$), mammographically or clinically positive ($n=78$), poor DW-MRI image quality ($n=9$), and missing pathology data on tumor characteristics ($n=14$) in the contralateral breast. Finally, 1130 women (mean age 53.3 ± 10.9 [standard deviation (SD)] years; range 26–84 years) were included (Fig. 1). Diagnosed index breast cancers were invasive carcinoma in 1016 women and ductal carcinoma in situ (DCIS) in 114 women.

MRI acquisition

All MRI examinations were performed in the prone position using two 3.0 T scanners (Skyra, Siemens Medical Solutions, Erlangen, Germany; Ingenia Cx, Philips Medical Systems, Best, the Netherlands) with a dedicated 18-channel breast coil. Details of MRI sequences are described in Appendix E1 and Table E1 (online). DW-MRI was acquired using rs-EPI sequence (RESOLVE, Siemens) or single-shot EPI sequence with parallel imaging (Sensitivity Encoding [SENSE], Philips); fat suppression; *b* values, 0 and 1000 s/mm^2. Repetition time [TR]/echo time [TE] was 8880/63 and 9194/93 ms (ms); section thickness of 3 mm; in-plane resolution of 1.8×1.8 mm and 1.2×1.2 mm; scanning time was 4 min 37 s and 2 min 46 s, respectively.

Readers and interpretation algorithm

Three radiologists (S.M.H, S.H.L, J.M.C, with 6, 8, and 13 years of experience in breast imaging, respectively) participated as readers. All readers were blinded to additional imaging, clinical, and histologic findings, except for the laterality of index cancer (right or left). Image analysis was performed by using data sets consisting of DW-MRI (*b* values, 0 and 1,000 s/mm^2 images and ADC

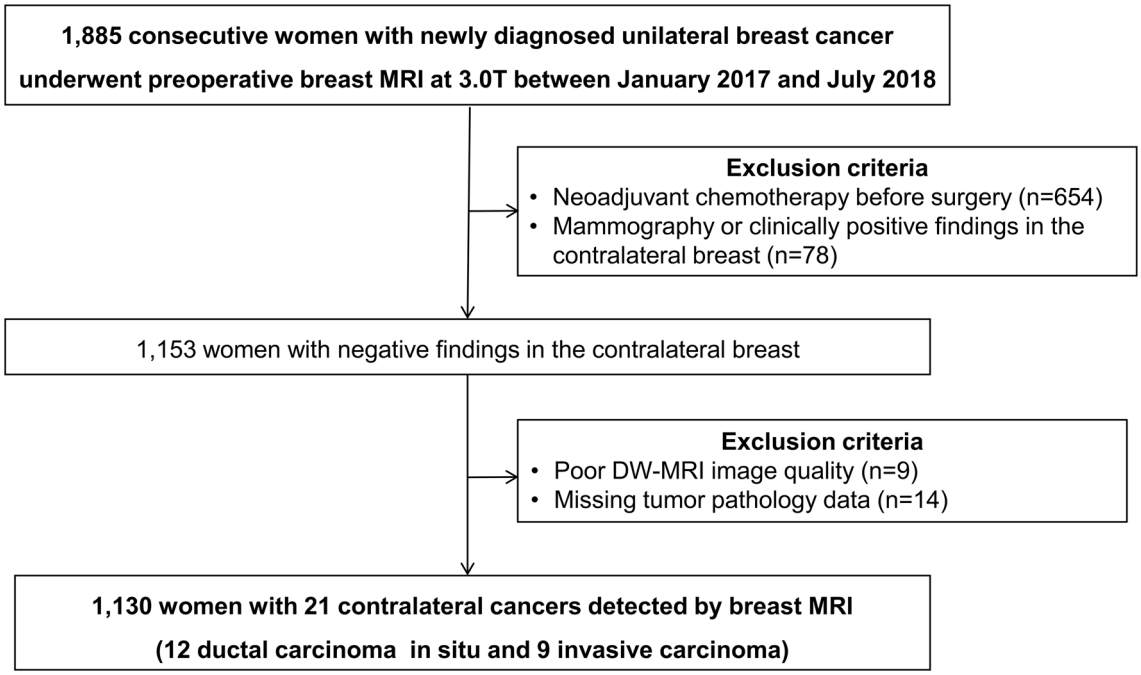

Fig. 1 Flow chart of the study population

maps) alone and DCE-MRI (DCE images and T1- and T2-weighted images) alone. ADC value was measured by small (3–6 mm^2) regions of interest within the darkest part of the lesion's ADC map using a PACS software (M-view, INFINITT Healthcare).

Before the reader study, three readers had an image training period with instructions about the DW-MRI interpretation algorithm (Fig. 2), using 50 sets of DW-MRI and DCE-MRI, which were not included in our study analysis. First, any unique areas of high signal intensity was identified on

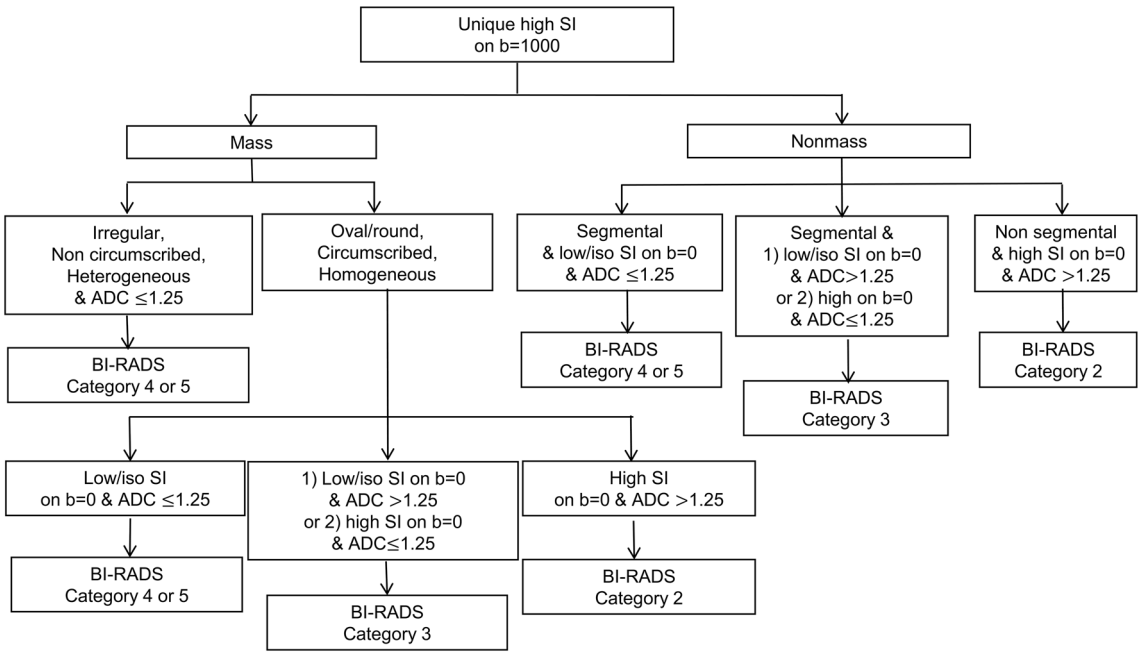

Fig. 2 Interpretation algorithm of diffusion-weighted MRI. *ADC* apparent diffusion coefficient, *BI-RADS* breast imaging reporting and data system, *SI* signal intensity

DW-MRI (b value of 1000 s/mm^2) and classified into mass or non-mass lesion. A mass was defined as suspicious if irregular shape, non-circumscribed margin, heterogeneous internal signal pattern, and low ADC value ($\leq 1.25 \times 10^{-3}$ mm^2/sec) [37]. A non-mass lesion was defined as suspicious if low to iso-signal intensity on DW-MRI (b value of 0 s/mm^2), segmental distribution, and low ADC value ($\leq 1.25 \times 10^{-3}$ mm^2/sec) [37]. Breast imaging reporting and data system (BI-RADS) category 1, negative or 2, benign assessment was given for DW-MRI examinations without any hyperintense lesion or hyperintense lesion without any suspicious finding, while BI-RADS category 3, probably benign; 4, suspicious; and 5, highly suggestive of malignancy assessment was given for DW-MRI examinations with more than one suspicious finding. DW-MRI interpretation algorithm for the specific application of unenhanced screening was developed based on the previous studies [19, 32, 37–39]. DCE-MRI diagnostic criteria were used in accordance with the 5th edition of BI-RADS MRI lexicon [40].

Reader study

After the training period, all three readers independently evaluated all DW-MRI and DCE-MRI ($n = 1130$) in a randomized counterbalanced way, half of our study cohort starting with DCE-MRI alone and the other half with DW-MRI alone. The readers were blinded to their own DW-MRI or DCE-MRI interpretation at the time of analysis. A non-blinded breast radiologist who was not involved in the reader study tracked lesions detected by at least one of three readers for correlation of identical lesions at both DW-MRI and DCE-MRI to assure the final evaluation of identical lesions in the statistical analysis after the readouts and measured quantitative ADC (Appendix E1 and Table E2 [online]).

Reference standard

The reference standard for each lesion was determined from the results of image-guided biopsy, surgery, and at least 1 year of clinical or imaging follow-up. When the lesion was detected only on DW-MRI without correlating lesion on DCE-MRI, the final diagnosis was determined from clinical or imaging follow-up. In case of a high-risk lesion (regarded as benign), the final diagnosis was established with surgery. A malignancy was defined as an invasive carcinoma or DCIS. We recorded the pathologic size and histologic features of benign and malignant lesions. For invasive carcinomas, lymph node status, histologic grade and expressions of estrogen (ER) and progesterone receptors (PR), and human epidermal growth factor receptor type 2 (HER2) were provided (Appendix E1 [online]). For DCIS, nuclear grade (low, intermediate, high) was recorded. Regardless of assessment by the readers in our study, clinical management was based on integrated interpretation of both DCE-MRI and DW-MRI findings.

Statistical analysis

To compute the diagnostic performance, BI-RADS category was dichotomized as follows: negative (BI-RADS category 1 or 2) or positive (BI-RADS category 3, 4, or 5), provided that the recommendation was other than routine screening [41]. The cancer detection rate was calculated as the number of true-positive cancers per 1000 examination. We stratified cancer detection rate by histologic type (DCIS or invasive cancers), size (≤ 1 cm or > 1 cm measured on DCE-MRI), and lesion type (mass or non-mass) and computed the rate ratio (defined as rate of DW-MRI/rate of DCE-MRI). Abnormal interpretation rate was defined as the proportion of lesions interpreted as BI-RADS category 3, 4, or 5. Sensitivity, specificity, positive predictive value (PPV), and negative predictive value (NPV), accuracy, and area under the curve (AUC) were measured. Due to the exploratory nature of our study, we compared performance of DW-MRI and DCE-MRI without correction for multiple comparisons. The inter-reader agreement for BI-RADS assessment was evaluated using κ statistic. The threshold for statistical significance was set at $P < 0.05$. All statistical analyses were performed using SPSS software, version 14.0 (IBM, Corp., Armonk, New York) (Appendix E1 [online]).

Results

Patient and tumor characteristics

Patient and detected cancer characteristics are shown in Tables 1 and 2, respectively. Among 1130 patients (mean age 53.3 ± 10.9 years, range 26–84 years), a total of 21 (1.9%, 21/1130) contralateral breast cancer were diagnosed by ultrasound-guided ($n = 11$) or MRI-guided needle biopsy ($n = 1$) and surgery ($n = 9$). All cancers were originally detected in clinical preoperative MRI examinations. The malignancies were invasive ductal carcinoma in 42.9% (9/21) and DCIS in 57.1% (12/21). The mean size of nine invasive tumors measured on pathologic specimens was 8 mm (range 1–20 mm) and none of the cancers were associated with lymph node metastasis (Table E3 [online]). The mean size of 21 DCIS on pathologic specimens was 23 mm (range 2–54 mm). Histology of benign lesions in 65 women including nine high-risk lesions (e.g., atypical ductal hyperplasia, atypical lobular hyperplasia, lobular carcinoma in situ) is provided in Table E4 (online).

Table 1 Characteristics of study cohort

Characteristics	Women with contralateral cancer ($n=21$)	Women without contralateral cancer ($n=1109$)	Total ($n=1130$)
Age, mean (SD) (years)	52.4 (11.1)	53.3 (11.0)	53.3 (10.9)
Median [range] (years)	52 [31–77]	52 [26–84]	52 [26–84]
Menopausal status			
Premenopausal or perimenopausal	9 (42.9)	450 (40.6)	459 (40.6)
Postmenopausal	12 (57.1)	659 (59.4)	671 (59.4)
Family history of breast cancer			
Absent	20 (95.2)	940 (84.8)	960 (85.0)
Present	1 (4.8)	169 (15.2)	170 (15.0)
Mammographic breast density			
Fatty or scattered fibroglandular	1 (4.8)	215 (19.4)	216 (19.1)
Heterogeneously or extremely dense	20 (95.2)	894 (80.6)	914 (80.9)

Data in parentheses are percentages

SD standard deviation

Abnormal interpretation rate and cancer detection rates

On the basis of positive DW-MRI reading, the abnormal interpretation rate of three readers was 12.6–16.2% with mean of 14.0% (95% CI [12.3, 15.7]) (Table 3). DW-MRI resulted in the cancer detection rate of 13–15 with mean of 14 per 1000 (95% CI [9–23 per 1000]). DCE-MRI resulted in a significantly higher abnormal interpretation rate of 14.2–19.0% with mean of 17.0% (95% CI [15.2, 18.9], $P=0.001$) and the cancer detection rate of 18–19 with mean of 18 per 1000 (95% CI [12–27 per 1000], $P=0.01$). For all three readers, mean cancer detection rate was significantly lower for DCIS (8 versus 10 per 1000, $P=0.04$) and lesions larger than 1 cm (8 versus 10 per 1000, $P=0.03$) on DW-MRI compared to that of DCE-MRI (Table 4). However, comparable cancer detection rates were achieved for invasive cancers (6 versus 8 per 1000, $P=0.15$). In addition, subgroup analysis according to the lesion type showed no significant difference in cancer detection rate of DW-MRI and DCE-MRI for all three readers; mass (11 versus 13 per 1000, $P=0.08$) and non-mass (4 versus 5 per 1000, $P=0.05$). DCE-MRI showed higher cancer detection rate than DW-MRI in lesions measuring less than 1 cm; however, it was statistically not significant (7 versus 8 per 1000, $P=0.17$).

Diagnostic performance and inter-reader agreement

DCE-MRI was more sensitive with an average of 96.8% (95% CI [88.7, 99.2]) compared to DW-MRI (77.8%, 95% CI [59.8, 89.2], $P<0.001$) (Table 3). The specificity of DW-MRI was 87.3% (95% CI [85.6, 88.8]), which was higher than DCE-MRI (84.6%, 95% CI [82.7, 86.2], $P<0.001$). The AUC of DW-MRI and DCE-MRI were 0.82 (95% CI [0.77, 0.87]) and 0.90 (95% CI [0.88, 0.92]), respectively. For both DW-MRI and DCE-MRI, NPV was high, 99.5% and 99.9%, respectively. There was substantial agreement between readers for BI-RADS assessment category for DW-MRI ($\kappa=0.87$) and DCE-MRI ($\kappa=0.95$).

False-negative and false-positive findings on DW-MRI

Of the 21 cancers, 14 (66.7%) were detected by all three reader and seven cancers (invasive ductal carcinoma [$n=2$] and DCIS [$n=5$]) were missed by at least one reader on DW-MRI; 2 (9.5%) missed by all readers, 3 (14.3%) by two reader, and 2 (9.5%) by one reader (Fig. 3). Two of the 21 cancers (9.5%) missed by all readers included one low-grade invasive cancer assessed as BI-RADS category 1 (Fig. 4) and one intermediate-grade, papillary DCIS assessed as BI-RADS category 2 (Fig. 5). The pathologic size of missed invasive cancer was 4 mm and presented as a 5 mm irregular mass on DCE-MRI, while the pathologic size of missed DCIS was 20 mm and presented as a 10 mm cystic mass with high ADC value on DW-MRI and rim enhancement on DCE-MRI.

False-positive findings on DW-MRI comprised 24, 27, and 26 lesions from readers 1, 2, and 3. Common false-positive findings assessed by all readers on DW-MRI included a range of features including seven high-risk lesions, four fibrocystic changes, two columnar cell changes, one nodular adenosis, and one duct ectasia with chronic inflammation. The mean ADC value encountered in these false-positive lesions was $1.04 \pm 0.63 \times 10^{-3}$ mm^2/s (range, $0.46–1.43 \times 10^{-3}$ mm^2/s) (Fig. 6).

Table 2 Characteristics of 21 detected cancers by MRI in the contralateral breast

Variables	No. (%)
No. of contralateral cancers	21
DCIS	12 (57.1)
Size of DCIS, mean [range] (mm)[a]	23 (2–54)
Invasive	9 (42.9)
Size of invasive tumor, mean [range] (mm)[a]	8 [1–20]
Node positive	0
Age (years)	
< 50	9 (42.9)
≥ 50	12 (57.1)
Lesion type	
Mass	15 (71.4)
Non-mass	6 (28.6)
Cancer type, grade and receptor status	
IDC, histologic grade	
High	1 (11.1)
Intermediate	5 (55.6)
Low	3 (33.3)
DCIS, nuclear grade	
High	2 (16.6)
Intermediate	5 (41.7)
Low	5 (41.7)
Estrogen receptor status	
Positive	17 (81.0)
Negative	2 (9.5)
Unknown	2 (9.5)
Progesterone receptor status	
Positive	16 (76.2)
Negative	3 (14.3)
Unknown	2 (9.5)
HER2 status	
Positive	1 (4.8)
Negative	18 (85.7)
Unknown	2 (9.5)

Data in parentheses are percentages

DCIS ductal carcinoma in situ, *HER2* human epidermal growth factor receptor type, *IDC* invasive ductal cancer

[a]Pathologic size

Discussion

Our study suggests that DW-MRI with optimized image acquisition and standardized interpretation algorithm has the potential to be an option for evaluation of contralateral breast in women with newly diagnosed breast cancer after negative mammography. In the blinded reader study of 1130 women with newly diagnosed unilateral breast cancer, DW-MRI at 3.0 T detected 14 mammographically occult cancers compared to 18 mammographically occult cancers per 1000 with DCE-MRI ($P = 0.01$) but with lower abnormal interpretation rate (14.0% versus 17.0%, $P = 0.001$) in the contralateral breast.

Increased concern about the accumulation of gadolinium-containing contrast agents necessitates unenhanced breast MRI protocol for breast cancer screening [19, 42]. Unenhanced DW-MRI has the potential to become a safer and cost-effective supplementary screening modality. However, at this time, limited studies have explored its utility and clinical use of DW-MRI alone for screening. Our breast MRI performance including incremental cancer detection rate, abnormal interpretation rate, and tumor characteristics is within the range of previous reports in women at elevated risk of breast cancer [4, 14, 43]. More than half of MRI-detected cancer were DCIS and invasive cancer were all node-negative T1 tumors, and the sensitivity of DW-MRI was lower but almost 80.0% of that of DCE-MRI (77.8% vs 96.8% $P < 0.001$). As awareness and concerns of gadolinium-containing contrast agents increase and as more personalized patient care are tailored, the efforts for breast cancer screening using DW-MRI are gaining momentum especially in intermediate-risk women. The use of DW-MRI as an alternative to DCE-MRI may have considerable impact regarding costs and availability of breast MRI examination.

Our study results were consistent with previous studies in which DW-MRI showed an overall lower sensitivity but higher specificity compared to DCE-MRI. Similar to our study design, there were several reader studies [28, 30–32, 44] in which DW-MRI was interpreted while blinded to DCE-MRI, reporting DW-MRI sensitivity average of 72.0% (range 45.0–94.0%) and specificity average of 90.0% (range 79.0–95.0%), both parameters from our study met at the higher end range. In three studies where DCE-MRI was considered as the reference standard with 100.0% sensitivity, DW-MRI sensitivity was reported to be average of 75.7% (range 46.0–77.0%) [28, 31, 44]. In two other studies comparing DW-MRI performance to mammography [32, 44], DW-MRI was more accurate than mammography alone for cancer detection (sensitivity 69.0% versus 40.0%, respectively) and the combination of mammography and DW-MRI improved sensitivity to 93.0% versus mammography or DW-MRI alone (64.0% and 74.0%, respectively). In a cancer-enriched cohort study including 48 women with 24 MRI-detected cancers, McDonald et al. [28] showed DW-MRI can reveal mammographically occult breast cancer with high specificity (91.0%) in women with dense breasts. However, although up to 71.0% of the cancers were visible, the mean sensitivity (45.0%) of DWI was notably lower than our study (77.8%). Recently, higher lesion visibility with DWI over ultrasound in detection of mammographically occult cancers has been reported [45]. Our study had several differences compared to previous studies regarding cancer prevalence, patient characteristics, and DW-MRI data acquisition and

Table 3 Performance of three readers with DW-MRI and DCE-MRI for the contralateral breast cancer detection in 1130 Women

MRI parameters	Readers	Cancer detection rate per 1000 (no./total) [95% CI]	Abnormal interpretation rate[a] (No./total) [95% CI]	Sensitivity (no./total) [95% CI]	Specificity (no./total) [95% CI]	PPV (no./total) [95% CI]	NPV (no./total) [95% CI]	Accuracy (no./total) [95% CI]	AUC [95% CI]
DW-MRI	R1	15.0 (17/1130) [9, 24]	12.6% (142/1130) [10.8, 14.6]	81.0% (17/21) [58.8, 92.7]	88.7% (984/1109) [86.7, 90.5]	12.0% (17/142) [7.6, 18.4]	99.6% (984/988) [98.9, 99.8]	88.6% (1001/1130) [86.6, 90.3]	0.84 [0.76,0.93]
	R2	15.0 (17/1130) [9, 24]	16.2% (183/1130) [14.2, 18.5]	81.0% (17/21) [58.8, 92.7]	85.0% (943/1109) [82.8, 87.0]	9.3% (17/183) [5.9, 14.4]	99.6% (943/947) [98.9, 99.8]	85.0% (960/1130) [82.8, 86.9]	0.82 [0.74, 0.91]
	R3	13.0 (15/1130) [8, 22]	13.1% (148/1130) [11.2, 15.2]	71.4% (15/21) [49.2, 86.6]	88.0% (976/1109) [86.0, 89.8]	10.1% (15/148) [6.2, 16.1]	99.4% (976/982) [98.6, 99.7]	87.7% (991/1,130) [85.7, 89.5]	0.79 [0.69, 0.89]
	Mean	14.0 [9, 23]	14.0% [12.3, 15.7]	77.8% [59.8, 89.2]	87.3% [85.6, 88.8]	10.4% [6.6, 15.9]	99.5% [98.9, 99.8]	87.1% [85.4, 88.6]	0.82 [0.77, 0.87]
DCE-MRI	R1	19.0 (21/130) [12, 28]	14.2% (161/1130) [12.3, 16.4]	100.0% (21/21) [100.0]	87.4% (969/1109) [85.3, 89.2]	13.0% (21/161) [8.7, 19.2]	100.0% (969/969) [100.0]	87.6% (990/1130) [85.6, 89.4]	0.93 [0.92, 0.94]
	R2	18.0 (20/1130) [11, 27]	19.0% (215/1130) [16.8, 21.4]	95.2% (20/21) [72.9,99.3]	82.4% (914/1109) [80.1, 84.5]	9.3% (20/215) [6.1, 14.0]	99.9% (914/915) [99.2, 100.0]	82.7% (934/1130) [80.3, 84.8]	0.88 [0.84, 0.93]
	R3	18.0 (20/1130) [11, 27]	17.6% (199/1130) [15.5, 19.9]	95.2% (20/21) [74.7,99.3]	83.9% (930/1109) [81.6, 85.9]	10.1% (20/199) [6.6, 15.1]	99.9% (930/931) [99.2, 100.0]	84.1% (950/1130) [81.8, 86.1]	0.89 [0.84, 0.93]
	Mean	18.0 [12, 27]	17.0% [15.2, 18.9]	96.8% [88.7, 99.2]	84.6% [82.7, 86.2]	10.6% [7.0, 15.7]	99.9% [99.7, 100.0]	84.8% [83.0, 86.4]	0.90 [0.88, 0.92]
P value	DW-MRI vs DCE-MRI	0.01†	0.001†	< 0.001†	< 0.001†	0.81	< 0.001†	< 0.001†	< 0.001†

Data in brackets are 95% confidence intervals and data in parentheses are numerator/denominator

AUC area under the curve, *CI* confidence interval, *DCE* dynamic contrast enhanced, *DW* diffusion-weighted, *NPV* negative predictive value, *PPV* positive predictive value, *R* reader

†*P* values less than 0.05 were considered to indicate a statistically significant difference

[a]As classified by using BI-RADS category 3, 4, or 5

interpretation [28, 30–32, 44]. Previous studies included asymptomatic screening patients and/or healthy controls [28, 30–32, 44], but with relatively high cancer prevalence (25.0–67.0%), in contrast to 1.9% in our study. An acquisition at 3.0 T with rs-EPI or EPI with parallel imaging and b value of 1000 s/mm^2 in our study allows high-resolution (1.2 × 1.2 mm and 1.8 × 1.8 mm in-plane resolution) DW-MRI images [46]. However, for screening applications, acquiring an additional very high *b* value of 1200–1500 s/mm^2 is recommended to maximize lesion contrast. Acquisition including three *b* values may be optimal for screening, with minimum b value of 0–50 s/mm^2, moderate *b* value of 800 s/mm^2 for quantification, and maximum of 1500 s/mm^2 for qualitative lesion detection [19, 46, 47]. The use of standardized interpretation algorithm and training of readers prior to study resulted high inter-reader agreement of DW-MRI in our study. However, there still is a need for dedicated training in DW-MRI alone interpretation considering our wider range of mean sensitivity with 59.8%-89.2% CI compared to DCE-MRI. With more validation of standardized interpretation algorithm and training for DW-MRI alone, we expect unenhanced DW-MRI a supplementary modality

Table 4 Cancer Detection Rate of DW-MRI and DCE-MRI according to Tumor Characteristics

Tumor characteristics	Cancer detection rate per 1000									
	R1		R2		R3		Mean		With DCE-MRI as reference	
	DW-MRI	DCE-MRI	DW-MRI	DCE-MRI	DW-MRI	DCE-MRI	DW-MRI	DCE-MRI	Rate ratio (95% CI)	*P* value
Size[a]										
≤ 1 cm ($n=10$)	7.0 (8)	9.0 (10)	7.0 (8)	8.0 (9)	6.0 (7)	8.0 (9)	7.0	8.0	0.82 [0.60, 1.08]	0.17
> 1 cm ($n=11$)	8.0 (9)	10.0 (11)	8.0 (9)	10.0 (11)	7.0 (8)	10.0 (11)	8.0	10.0	0.78 [0.63, 0.98]	0.03[†]
Cancer type										
Invasive ($n=9$)	6.0 (7)	8.0 (9)	6.0 (7)	7.0 (8)	7.0 (8)	8.0 (9)	6.0	8.0	0.84 [0.67, 1.06]	0.15
DCIS ($n=12$)	9.0 (10)	11.0 (12)	9.0 (10)	11.0 (12)	6.0 (7)	10.0 (11)	8.0	10.0	0.77 [0.59, 0.99]	0.04[†]
Lesion type										
Mass ($n=15$)	12.0 (13)	13.0 (15)	11.0 (12)	12.0 (14)	10.0 (11)	12.0 (14)	11.0	13.0	0.83 [0.67, 1.02]	0.08
Non-mass ($n=6$)	3.0 (4)	5.0 (6)	4.0 (5)	5.0 (6)	3.0 (4)	5.0 (6)	4.0	5.0	0.72 [0.51, 1.01]	0.05

Data in brackets are 95% confidence intervals and values are rate per 1000 with number of cancers in parenthesis

CI confidence interval, *DCE* dynamic contrast enhanced, *DCIS* ductal carcinoma in situ, *DW* diffusion-weighted, *R* reader

[†] *P* values less than 0.05 were considered to indicate a statistically significant difference

[a] Longest diameter on DCE-MRI

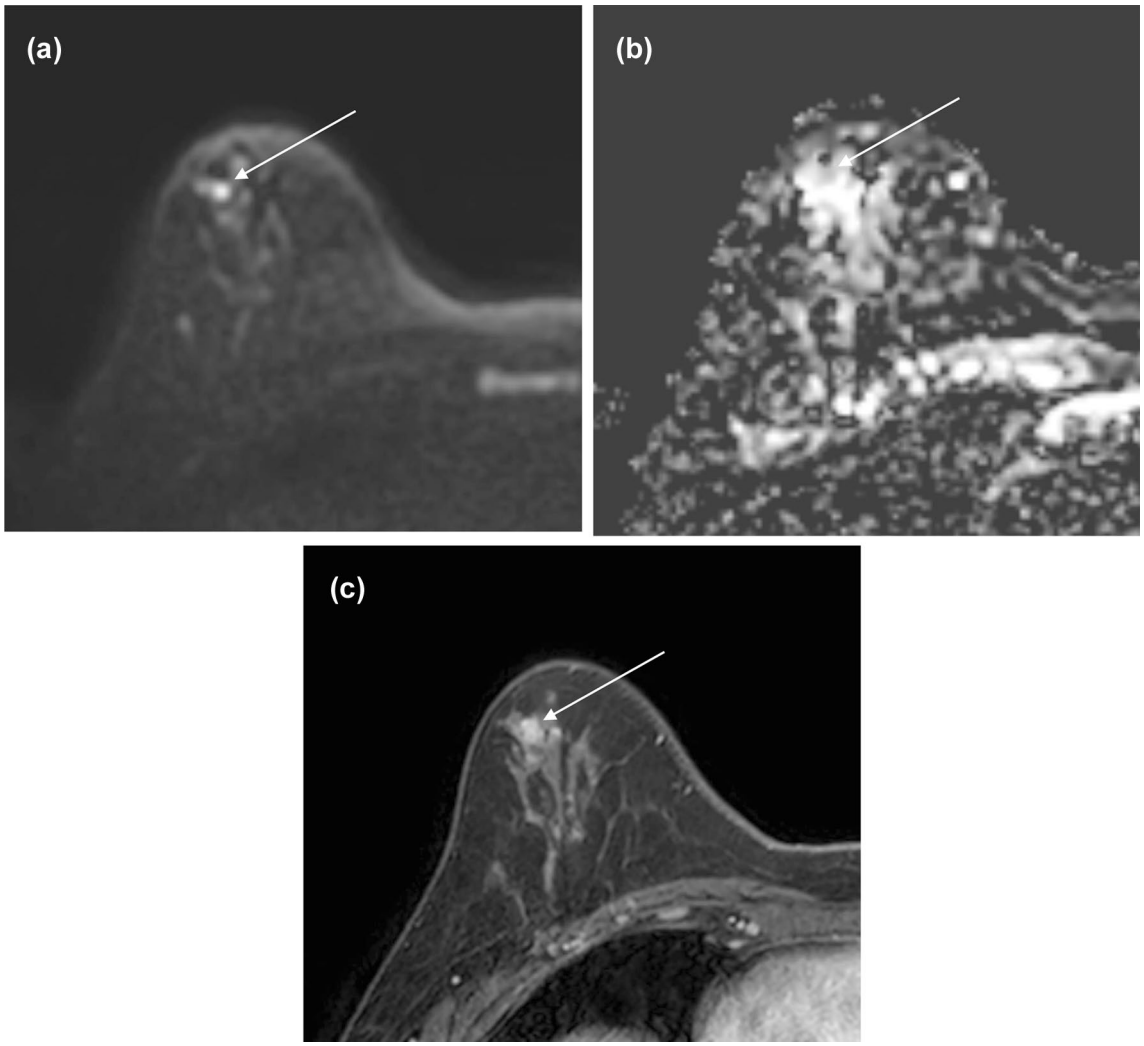

Fig. 3 A 44-year-old woman with invasive ductal carcinoma in the right breast. **a** Axial image from diffusion-weighted (DW)-MRI ($b = 1000$ s/mm^2) shows a round mass (arrow) with high signal intensity. **b** On the apparent diffusion coefficient (ADC) map, the mass (arrow) shows low mean ADC (1.02×10^{-3} mm^2/sec). **c** Axial T1-weighted subtraction image from dynamic contrast-enhanced (DCE)-MRI shows a 5 mm irregular heterogeneous enhancing mass (arrow). The mass was assessed as BI-RADS category 4, suspicious by all readers on both DW-MRI and DCE-MRI. Surgical histopathologic examination showed a 2 mm intermediate histologic grade invasive ductal carcinoma that was node negative, estrogen receptor positive, progesterone receptor positive, and human epidermal growth factor receptor 2 negative

for screening for breast cancer, beyond evaluation of extent of disease in women with newly diagnosed breast cancer.

In our study, a low-grade invasive cancer measured as 5 mm size on DCE-MRI was missed by all readers, assessed as BI-RADS category 1, negative and another papillary DCIS with cystic change on pathologic result, rim enhancement on DCE-MRI, and corresponding high ADC value was misclassified and assessed as BI-RADS category 2, benign. Literature suggests that DCIS and lesions less than 10–12 mm may be more difficult to detect at DW-MRI [48]. In our study, however, DW-MRI achieved comparable cancer detection rates for invasive cancers, lesions measuring less than ≤1 cm, although lower cancer detection rates were observed for DCIS. DCIS often manifesting as microcalcification or non-mass enhancement are mostly missed by DW-MRI compared to the invasive counterpart with a range of 0–40.0% [26–28, 30, 31, 48], which in our study, missed by at least one reader was 71.4% (5/7). In general, DCIS exhibits less diffusion impedance as reflected by higher ADC measurements, compared with invasive carcinoma, which may explain their relatively low conspicuity at DW-MRI. Indeed, there are mixed reports regarding correlation between ADC value and DCIS grade [49–51]. Also, cancers with necrosis or mucinous histology are missed because of their high ADC values [52]. We found ADC value discrimination ability of benign and malignant lesions was lower in

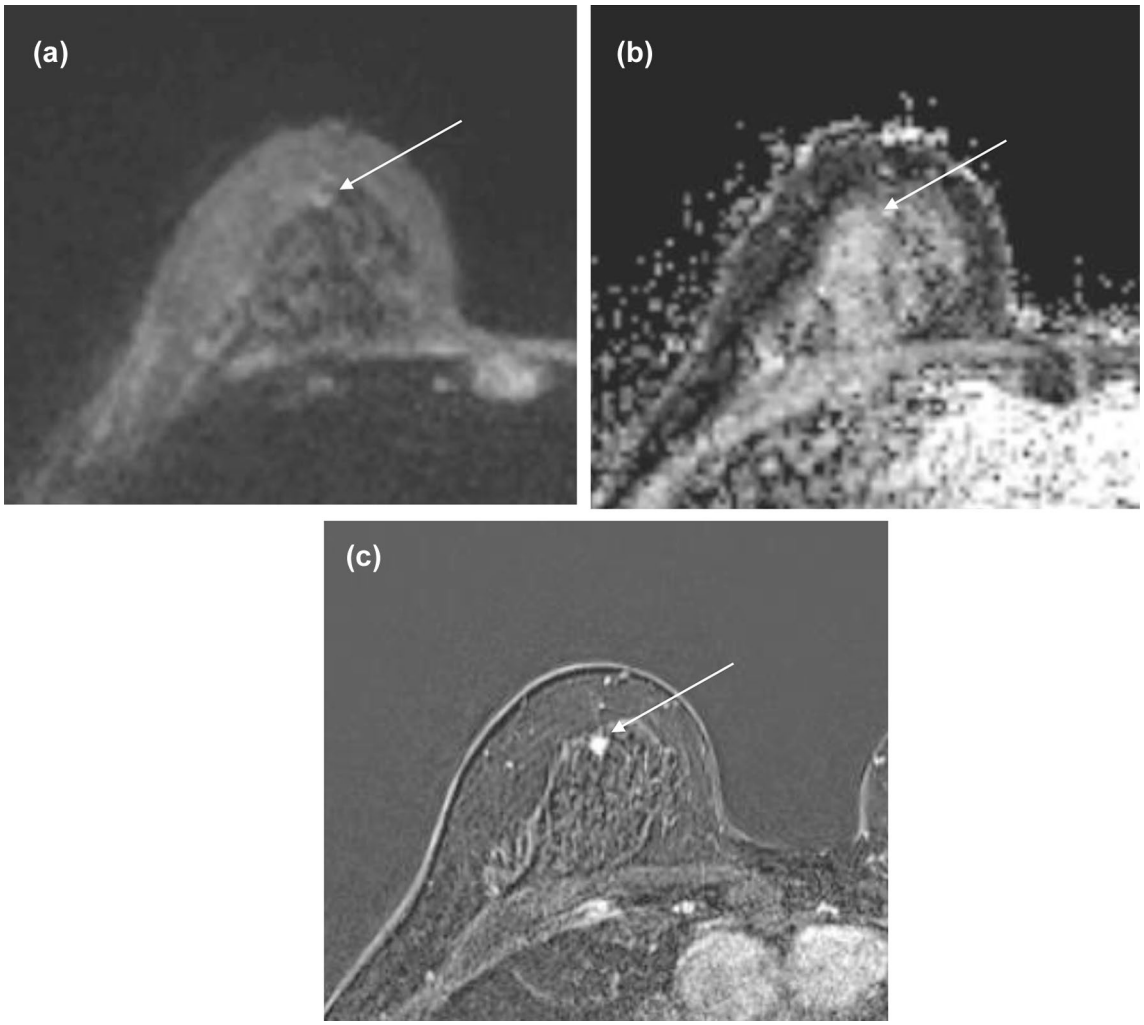

Fig. 4 A 56-year-old woman with invasive ductal carcinoma in the right breast. **a** Axial image from diffusion-weighted (DW)-MRI ($b = 1000$ s/mm^2) shows mildly elevated signal intensity (arrow). **b** On the apparent diffusion coefficient (ADC) map, the mass (arrow) shows low mean ADC (1.16×10^{-3} mm^2/sec). **c** Axial T1-weighted subtraction image from dynamic contrast-enhanced (DCE)-MRI shows a 5 mm enhancing mass with irregular margin (arrow). The mass was missed by all three readers in blinded reader study on DW-MRI. Surgical histopathologic examination showed a 4 mm low histologic grade invasive ductal carcinoma that was node negative, estrogen receptor positive, progesterone receptor positive, and human epidermal growth factor receptor 2 negative

larger than 1 cm lesions, mainly due to non-mass lesions [53]. The most common false-positive findings assessed by all readers on DW-MRI were high-risk lesions in our study. In the literature, complicated/proteinaceous cysts, fibroadenoma, and artifactual lesions are commonly reported false-positive lesions at DW-MRI [28].

Our study had several limitations. First, a bias on patient selection might have occurred because of the retrospective study design. Also due to retrospective study design, DW-MRI alone detected lesions could not be pathologically confirmed. With relatively small number of malignant lesions and short-term follow-up period of at least 1 year in our study, we cannot exclude the possibility that a longer follow-up could reveal additional malignant lesions. Further investigation and validation in larger studies with longer follow-up period are warranted. Second, our results obtained in the screening setting of the contralateral breast in women with newly diagnosed breast cancer may not be generalized to other screening indications. Third, two 3.0T MRI scanners from different vendors were used. Image quality and ADC value measurement may not be the same across vendors [54, 55]. Fourth, maximum intensity projections techniques were not used for DW-MRI image display. DW-MRI with maximum intensity projections can reduce reading time and allow for comparable analysis approach to that used for abbreviated contrast-enhanced MRI protocols [56]. Fifth, due to the exploratory nature of our study, we compared performance of DW-MRI and DCE-MRI without correction for multiple comparisons. In addition, in our study, DCE-MRI may have resulted higher cancer detection rate than DW-MRI

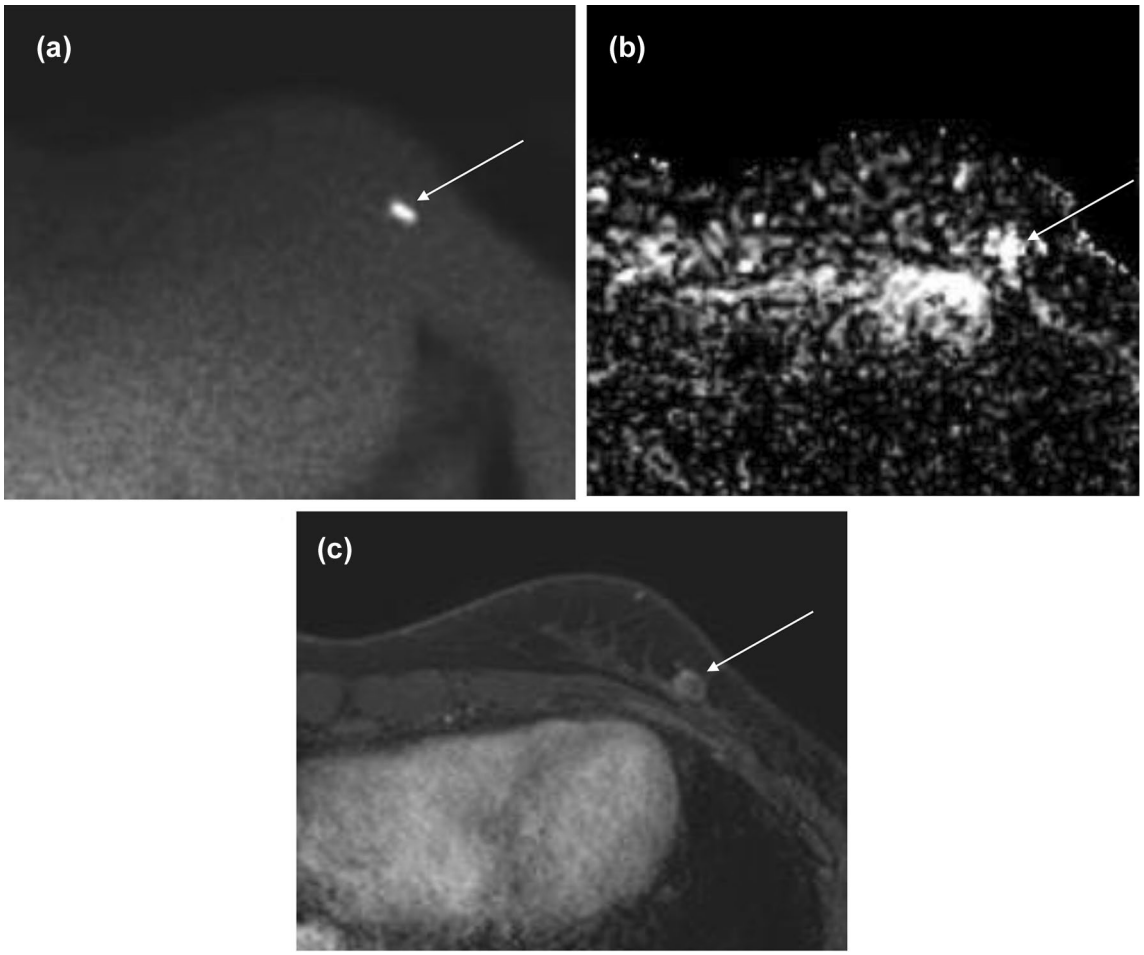

Fig. 5 A 42-year-old woman with intermediate-grade ductal carcinoma in situ in the left breast. **a** Axial image from diffusion-weighted (DW)-MRI ($b = 1000$ s/mm^2) shows an ovoid mass (arrow) with high signal intensity. **b** On the apparent diffusion coefficient (ADC) map, the mass (arrow) shows high mean ADC (2.50×10^{-3} mm^2/sec). The mass was assessed as BI-RADS category 2, benign by all readers. **c** Axial T1-weighted subtraction image from dynamic contrast-enhanced (DCE)-MRI shows a 10 mm rim-enhancing mass (arrow), assessed as BI-RADS category 4, suspicious by all readers. The DW-MRI was false-negative for this patient. Histopathology result reveals a 20 mm papillary DCIS with cystic change

due to higher spatial resolution. Lastly, performance of DW-MRI was not compared with other supplemental imaging modalities including ultrasound. However, incremental cancer detection rate of digital breast tomosynthesis and ultrasound after mammography is reported 1.1–2.9 (mean 1.6) and 1.8–4.6 (mean 2.3) per 1000 examinations, respectively [57, 58], and DW-MRI may detect more breast cancers than combined digital breast tomosynthesis and ultrasound [45, 58]. A multi-center prospective screening trial comparing the sensitivity of mammography, ultrasound, DCE-MRI, and DW-MRI for detection of breast cancers is undergoing in women at high risk and optimal approach for screening using readily available techniques is proposed recently [59].

In conclusion, DW-MRI of the contralateral breast in women with newly diagnosed breast cancer has lower cancer detection rate and sensitivity but lower abnormal interpretation rate and higher specificity compared with DCE-MRI. Our results suggest that given the acceptable performance, short scan time, and lack of contrast agent-associated risks, DW-MRI at 3.0T has the potential as a cost-effective tool for evaluation of contralateral breast in women with newly diagnosed breast cancer. DW-MRI may be an alternative option in patients with contraindications to gadolinium-based contrast agents. Optimized image acquisition, use of standardized interpretation algorithm, and dedicated training in DW-MRI interpretation are important to ensure reliable sensitivity and specificity. Multi-center prospective trials are needed to better determine the value of DW-MRI as a stand-alone screening tool.

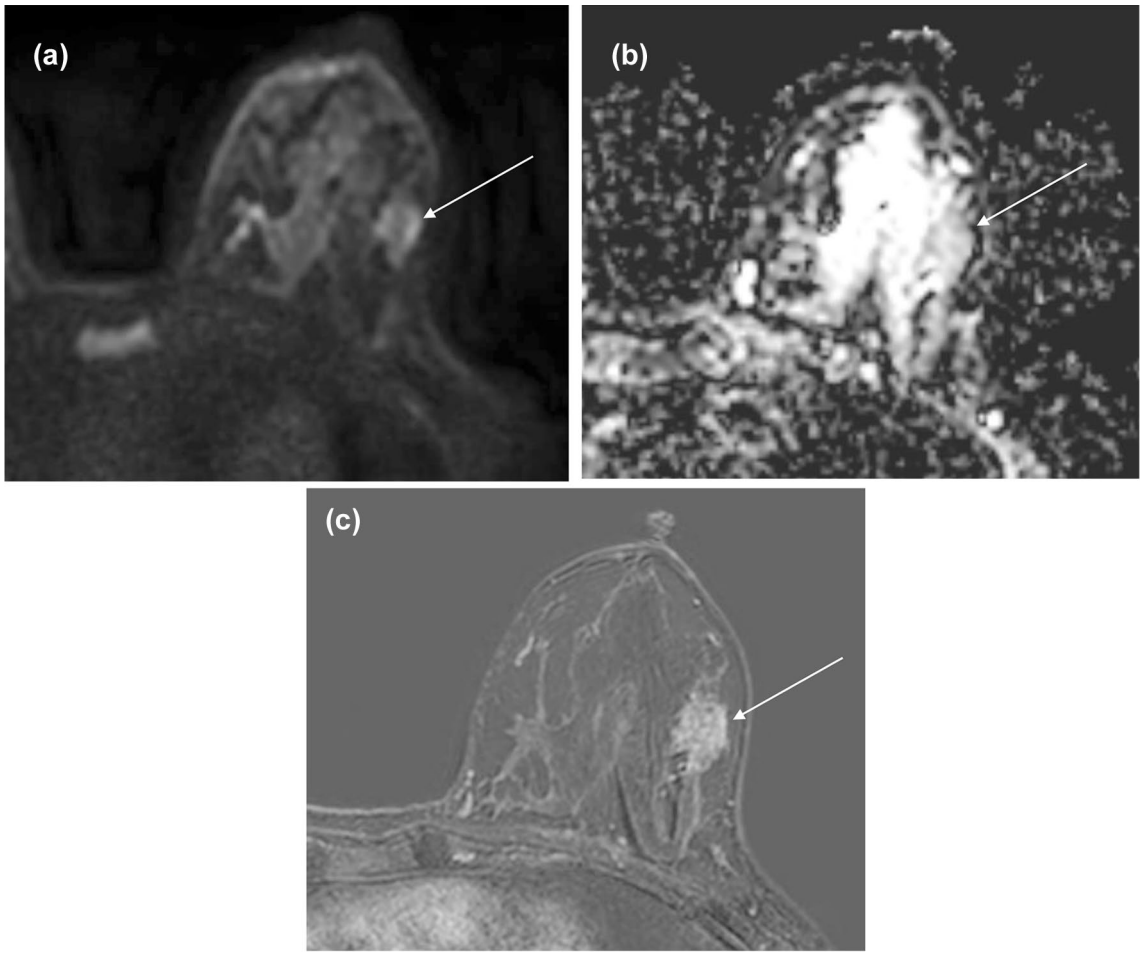

Fig. 6 A 40-year-old woman with stromal fibrosis in the left breast. **a** Axial image from diffusion-weighted (DW)-MRI ($b = 1000$ s/mm^2) shows non-mass lesion with high signal intensity (arrow). **b** On the apparent diffusion coefficient (ADC) map, the lesion (arrow) shows low mean ADC (1.10×10^{-3} mm^2/sec). **c** Axial T1-weighted subtraction image from dynamic contrast-enhanced (DCE)-MRI shows heterogeneous non-mass enhancement (arrow). The lesion was false positive on both DWI-MRI and DCE-MRI, assessed as BI-RADS category 3, probably benign or 4, suspicious by all readers

Acknowledgement We thank Kim, Na Young, a statistician who helped with statistics.

Funding This research was supported by a grant of the Korea Health Technology R&D Project through the Korea Health Industry Development Institute (KHIDI), funded by the Ministry of Health and Welfare (Grant Number: HI15C1532), and the National R&D Program for Cancer Control, Ministry of Health and Welfare, Republic of Korea (Grant Number: HA17C0056).

Compliance with ethical standards

Conflict of interest All authors declare that they have no conflict of interest.

Ethical approval All procedures performed in studies involving human participants were in accordance with the ethical standards of the institutional committee and with the 1964 Helsinki declaration and its later amendments or comparable ethical standards.

Informed Consent This retrospective study was approved by the institutional review board, and the informed consent requirement was waived.

References

1. Oeffinger KC, Fontham ET, Etzioni R, Herzig A, Michaelson JS, Shih YC, Walter LC, Church TR, Flowers CR, LaMonte SJ, Wolf AM, DeSantis C, Lortet-Tieulent J, Andrews K, Manassaram-Baptiste D, Saslow D, Smith RA, Brawley OW, Wender R, American Cancer Society (2015) Breast cancer screening for women at average risk: 2015 guideline update from the American Cancer Society. JAMA 314:1599–1614. https://doi.org/10.1001/jama.2015.12783
2. Berg WA, Blume JD, Cormack JB, Mendelson EB, Lehrer D, Bohm-Velez M, Pisano ED, Jong RA, Evans WP, Morton MJ, Mahoney MC, Larsen LH, Barr RG, Farria DM, Marques HS, Boparai K, ACRIN 6666 Investigators (2008) Combined screening

with ultrasound and mammography vs mammography alone in women at elevated risk of breast cancer. JAMA 299:2151–2163. https://doi.org/10.1001/jama.299.18.2151
3. Mainiero MB, Moy L, Baron P, Didwania AD, diFlorio RM, Green ED, Heller SL, Holbrook AI, Lee SJ, Lewin AA, Lourenco AP, Nance KJ, Niell BL, Slanetz PJ, Stuckey AR, Vincoff NS, Weinstein SP, Yepes MM, Newell MS (2017) ACR appropriateness criteria® breast cancer screening. J Am Coll Radiol 14:S383–S390. https://doi.org/10.1016/j.jacr.2017.08.044
4. Brennan ME, Houssami N, Lord S, Macaskill P, Irwig L, Dixon JM, Warren RM, Ciatto S (2009) Magnetic resonance imaging screening of the contralateral breast in women with newly diagnosed breast cancer: systematic review and meta-analysis of incremental cancer detection and impact on surgical management. J Clin Oncol 27:5640–5649. https://doi.org/10.1200/jco.2008.21.5756
5. Lehman CD, Gatsonis C, Kuhl CK, Hendrick RE, Pisano ED, Hanna L, Peacock S, Smazal SF, Maki DD, Julian TB, DePeri ER, Bluemke DA, Schnall MD, ACRIN Trial 6667 Investigators Group (2007) MRI evaluation of the contralateral breast in women with recently diagnosed breast cancer. N Engl J Med 356:1295–1303. https://doi.org/10.1056/NEJMoa065447
6. Kuhl CK, Schrading S, Strobel K, Schild HH, Hilgers RD, Bieling HB (2014) Abbreviated breast magnetic resonance imaging (MRI): first postcontrast subtracted images and maximum-intensity projection-a novel approach to breast cancer screening with MRI. J Clin Oncol 32:2304–2310. https://doi.org/10.1200/JCO.2013.52.5386
7. Gweon HM, Cho N, Han W, Yi A, Moon HG, Noh DY, Moon WK (2014) Breast MR imaging screening in women with a history of breast conservation therapy. Radiology 272:366–373. https://doi.org/10.1148/radiol.14131893
8. Lehman CD, Lee JM, DeMartini WB, Hippe DS, Rendi MH, Kalish G, Porter P, Gralow J, Partridge SC (2016) Screening MRI in women With a personal history of breast cancer. J Natl Cancer Inst. https://doi.org/10.1093/jnci/djv349
9. Monticciolo DL, Newell MS, Moy L, Niell B, Monsees B, Sickles EA (2018) Breast cancer screening in women at higher-than-average risk: recommendations from the ACR. J Am Coll Radiol 15:408–414. https://doi.org/10.1016/j.jacr.2017.11.034
10. Houssami N, Hayes DF (2009) Review of preoperative magnetic resonance imaging (MRI) in breast cancer: should MRI be performed on all women with newly diagnosed, early stage breast cancer? CA Cancer J Clin 59:290–302. https://doi.org/10.3322/caac.20028
11. Lehman CD, Gatsonis C, Kuhl CK, Hendrick RE, Pisano ED, Hanna L, Peacock S, Smazal SF, Maki DD, Julian TB, DePeri ER, Bluemke DA, Schnall MD (2007) MRI evaluation of the contralateral breast in women with recently diagnosed breast cancer. N Engl J Med 356:1295–1303. https://doi.org/10.1056/NEJMoa065447
12. Morrow M, Waters J, Morris E (2011) MRI for breast cancer screening, diagnosis, and treatment. Lancet 378:1804–1811. https://doi.org/10.1016/s0140-6736(11)61350-0
13. Sardanelli F, Boetes C, Borisch B, Decker T, Federico M, Gilbert FJ, Helbich T, Heywang-Kobrunner SH, Kaiser WA, Kerin MJ, Mansel RE, Marotti L, Martincich L, Mauriac L, Meijers-Heijboer H, Orecchia R, Panizza P, Ponti A, Purushotham AD, Regitnig P, Del Turco MR, Thibault F, Wilson R (2010) Magnetic resonance imaging of the breast: recommendations from the EUSOMA working group. Eur J Cancer 46:1296–1316. https://doi.org/10.1016/j.ejca.2010.02.015
14. Lee JM, Ichikawa L, Valencia E, Miglioretti DL, Wernli K, Buist DSM, Kerlikowske K, Henderson LM, Sprague BL, Onega T, Rauscher GH, Lehman CD (2017) Performance Benchmarks for Screening Breast MR Imaging in Community Practice. Radiology 285:44–52. https://doi.org/10.1148/radiol.2017162033
15. Niell BL, Gavenonis SC, Motazedi T, Chubiz JC, Halpern EP, Rafferty EA, Lee JM (2014) Auditing a breast MRI practice: performance measures for screening and diagnostic breast MRI. J Am Coll Radiol 11:883–889. https://doi.org/10.1016/j.jacr.2014.02.003
16. Strigel RM, Rollenhagen J, Burnside ES, Elezaby M, Fowler AM, Kelcz F, Salkowski L, DeMartini WB (2017) Screening breast MRI outcomes in routine clinical practice: comparison to BI-RADS benchmarks. Acad Radiol 24:411–417. https://doi.org/10.1016/j.acra.2016.10.014
17. Houssami N, Turner RM, Morrow M (2017) Meta-analysis of pre-operative magnetic resonance imaging (MRI) and surgical treatment for breast cancer. Breast Cancer Res Treat 165:273–283. https://doi.org/10.1007/s10549-017-4324-3
18. Leithner D, Moy L, Morris EA, Marino MA, Helbich TH, Pinker K (2019) Abbreviated MRI of the breast: does it provide value? J Magn Reson Imaging 49:e85–e100. https://doi.org/10.1002/jmri.26291
19. Amornsiripanitch N, Bickelhaupt S, Shin HJ, Dang M, Rahbar H, Pinker K, Partridge SC (2019) Diffusion-weighted MRI for unenhanced breast cancer screening. Radiology 293:504–520. https://doi.org/10.1148/radiol.2019182789
20. Partridge SC, McDonald ES (2013) Diffusion weighted magnetic resonance imaging of the breast: protocol optimization, interpretation, and clinical applications. Magn Reson Imaging Clin N Am 21:601–624. https://doi.org/10.1016/j.mric.2013.04.007
21. Galban CJ, Ma B, Malyarenko D, Pickles MD, Heist K, Henry NL, Schott AF, Neal CH, Hylton NM, Rehemtulla A, Johnson TD, Meyer CR, Chenevert TL, Turnbull LW, Ross BD (2015) Multi-site clinical evaluation of DW-MRI as a treatment response metric for breast cancer patients undergoing neoadjuvant chemotherapy. PLoS ONE 10:e0122151. https://doi.org/10.1371/journal.pone.0122151
22. Baxter GC, Graves MJ, Gilbert FJ, Patterson AJ (2019) A meta-analysis of the diagnostic performance of diffusion MRI for breast lesion characterization. Radiology 291:632–641. https://doi.org/10.1148/radiol.2019182510
23. Woodhams R, Matsunaga K, Kan S, Hata H, Ozaki M, Iwabuchi K, Kuranami M, Watanabe M, Hayakawa K (2005) ADC mapping of benign and malignant breast tumors. Magn Reson Med Sci 4:35–42. https://doi.org/10.2463/mrms.4.35
24. Zhang L, Tang M, Min Z, Lu J, Lei X, Zhang X (2016) Accuracy of combined dynamic contrast-enhanced magnetic resonance imaging and diffusion-weighted imaging for breast cancer detection: a meta-analysis. Acta Radiol 57:651–660. https://doi.org/10.1177/0284185115597265
25. Rahbar H, Zhang Z, Chenevert TL, Romanoff J, Kitsch AE, Hanna LG, Harvey SM, Moy L, DeMartini WB, Dogan B, Yang WT, Wang LC, Joe BN, Oh KY, Neal CH, McDonald ES, Schnall MD, Lehman CD, Comstock CE, Partridge SC (2019) Utility of diffusion-weighted imaging to decrease unnecessary biopsies prompted by breast MRI: a trial of the ECOG-ACRIN Cancer Research Group (A6702). Clin Cancer Res 25:1756–1765. https://doi.org/10.1158/1078-0432.CCR-18-2967
26. Baltzer PA, Benndorf M, Dietzel M, Gajda M, Camara O, Kaiser WA (2010) Sensitivity and specificity of unenhanced MR mammography (DWI combined with T2-weighted TSE imaging, ueMRM) for the differentiation of mass lesions. Eur Radiol 20:1101–1110. https://doi.org/10.1007/s00330-009-1654-5
27. Bickelhaupt S, Laun FB, Tesdorff J, Lederer W, Daniel H, Stieber A, Delorme S, Schlemmer HP (2016) Fast and noninvasive characterization of suspicious lesions detected at breast cancer X-Ray screening: capability of diffusion-weighted MR imaging

with MIPs. Radiology 278:689–697. https://doi.org/10.1148/radiol.2015150425
28. McDonald ES, Hammersley JA, Chou SH, Rahbar H, Scheel JR, Lee CI, Liu CL, Lehman CD, Partridge SC (2016) Performance of DWI as a rapid unenhanced technique for detecting mammographically occult breast cancer in elevated-risk women with dense breasts. AJR Am J Roentgenol 207:205–216. https://doi.org/10.2214/AJR.15.15873
29. Shin HJ, Chae EY, Choi WJ, Ha SM, Park JY, Shin KC, Cha JH, Kim HH (2016) Diagnostic performance of fused diffusion-weighted imaging using unenhanced or postcontrast T1-weighted MR imaging in patients with breast cancer. Medicine (Baltimore) 95:e3502. https://doi.org/10.1097/MD.0000000000003502
30. Telegrafo M, Rella L, Stabile Ianora AA, Angelelli G, Moschetta M (2015) Unenhanced breast MRI (STIR, T2-weighted TSE, DWIBS): an accurate and alternative strategy for detecting and differentiating breast lesions. Magn Reson Imaging 33:951–955. https://doi.org/10.1016/j.mri.2015.06.002
31. Trimboli RM, Verardi N, Cartia F, Carbonaro LA, Sardanelli F (2014) Breast cancer detection using double reading of unenhanced MRI including T1-weighted, T2-weighted STIR, and diffusion-weighted imaging: a proof of concept study. AJR Am J Roentgenol 203:674–681. https://doi.org/10.2214/AJR.13.11816
32. Yabuuchi H, Matsuo Y, Sunami S, Kamitani T, Kawanami S, Setoguchi T, Sakai S, Hatakenaka M, Kubo M, Tokunaga E, Yamamoto H, Honda H (2011) Detection of non-palpable breast cancer in asymptomatic women by using unenhanced diffusion-weighted and T2-weighted MR imaging: comparison with mammography and dynamic contrast-enhanced MR imaging. Eur Radiol 21:11–17. https://doi.org/10.1007/s00330-010-1890-8
33. Kang JW, Shin HJ, Shin KC, Chae EY, Choi WJ, Cha JH, Kim HH (2017) Unenhanced magnetic resonance screening using fused diffusion-weighted imaging and maximum-intensity projection in patients with a personal history of breast cancer: role of fused DWI for postoperative screening. Breast Cancer Res Treat 165:119–128. https://doi.org/10.1007/s10549-017-4322-5
34. Bogner W, Pinker K, Zaric O, Baltzer P, Minarikova L, Porter D, Bago-Horvath Z, Dubsky P, Helbich TH, Trattnig S, Gruber S (2015) Bilateral diffusion-weighted MR imaging of breast tumors with submillimeter resolution using readout-segmented echo-planar imaging at 7 T. Radiology 274:74–84. https://doi.org/10.1148/radiol.14132340
35. Bogner W, Pinker-Domenig K, Bickel H, Chmelik M, Weber M, Helbich TH, Trattnig S, Gruber S (2012) Readout-segmented echo-planar imaging improves the diagnostic performance of diffusion-weighted MR breast examinations at 3.0 T. Radiology 263:64–76. https://doi.org/10.1148/radiol.12111494
36. Partridge SC, Demartini WB, Kurland BF, Eby PR, White SW, Lehman CD (2010) Differential diagnosis of mammographically and clinically occult breast lesions on diffusion-weighted MRI. J Magn Reson Imaging 31:562–570. https://doi.org/10.1002/jmri.22078
37. Bogner W, Gruber S, Pinker K, Grabner G, Stadlbauer A, Weber M, Moser E, Helbich TH, Trattnig S (2009) Diffusion-weighted MR for differentiation of breast lesions at 3.0 T: how does selection of diffusion protocols affect diagnosis? Radiology 253:341–351. https://doi.org/10.1148/radiol.2532081718
38. Kuroki-Suzuki S, Kuroki Y, Nasu K, Nawano S, Moriyama N, Okazaki M (2007) Detecting breast cancer with non-contrast MR imaging: combining diffusion-weighted and STIR imaging. Magn Reson Med Sci 6:21–27
39. Radovic N, Ivanac G, Divjak E, Biondic I, Bulum A, Brkljacic B (2019) Evaluation of breast cancer morphology using diffusion-weighted and dynamic contrast-enhanced MRI: intermethod and interobserver agreement. J Magn Reson Imaging 49:1381–1390. https://doi.org/10.1002/jmri.26332
40. D'Orsi CJ (2013) ACR BI-RADS atlas : breast imaging reporting and data system. American College of Radiology, Reston (VA)
41. Berg WA, Zhang Z, Lehrer D, Jong RA, Pisano ED, Barr RG, Bohm-Velez M, Mahoney MC, Evans WP 3rd, Larsen LH, Morton MJ, Mendelson EB, Farria DM, Cormack JB, Marques HS, Adams A, Yeh NM, Gabrielli G, ACRIN 6666 Investigators (2012) Detection of breast cancer with addition of annual screening ultrasound or a single screening MRI to mammography in women with elevated breast cancer risk. JAMA 307:1394–1404. https://doi.org/10.1001/jama.2012.388
42. Kanda T, Fukusato T, Matsuda M, Toyoda K, Oba H, Kotoku J, Haruyama T, Kitajima K, Furui S (2015) Gadolinium-based contrast agent accumulates in the brain even in subjects without severe renal dysfunction: evaluation of autopsy brain specimens with inductively coupled plasma mass spectroscopy. Radiology 276:228–232. https://doi.org/10.1148/radiol.2015142690
43. Cho N, Han W, Han BK, Bae MS, Ko ES, Nam SJ, Chae EY, Lee JW, Kim SH, Kang BJ, Song BJ, Kim EK, Moon HJ, Kim SI, Kim SM, Kang E, Choi Y, Kim HH, Moon WK (2017) Breast cancer screening with mammography plus ultrasonography or magnetic resonance imaging in women 50 years or younger at diagnosis and treated with breast conservation therapy. JAMA Oncol 3:1495–1502. https://doi.org/10.1001/jamaoncol.2017.1256
44. Kazama T, Kuroki Y, Kikuchi M, Sato Y, Nagashima T, Miyazawa Y, Sakakibara M, Kaneoya K, Makimoto Y, Hashimoto H, Motoori K, Takano H (2012) Diffusion-weighted MRI as an adjunct to mammography in women under 50 years of age: an initial study. J Magn Reson Imaging 36:139–144. https://doi.org/10.1002/jmri.23626
45. Amornsiripanitch N, Rahbar H, Kitsch AE, Lam DL, Weitzel B, Partridge SC (2018) Visibility of mammographically occult breast cancer on diffusion-weighted MRI versus ultrasound. Clin Imaging 49:37–43. https://doi.org/10.1016/j.clinimag.2017.10.017
46. Han X, Li J, Wang X (2017) Comparison and optimization of 3.0 T breast images quality of diffusion-weighted imaging with multiple b-values. Acad Radiol 24:418–425. https://doi.org/10.1016/j.acra.2016.11.006
47. Tamura T, Murakami S, Naito K, Yamada T, Fujimoto T, Kikkawa T (2014) Investigation of the optimal b-value to detect breast tumors with diffusion weighted imaging by 1.5-T MRI. Cancer Imaging 14:11. https://doi.org/10.1186/1470-7330-14-11
48. Pinker K, Moy L, Sutton EJ, Mann RM, Weber M, Thakur SB, Jochelson MS, Bago-Horvath Z, Morris EA, Baltzer PA, Helbich TH (2018) Diffusion-weighted imaging with apparent diffusion coefficient mapping for breast cancer detection as a stand-alone parameter: comparison with dynamic contrast-enhanced and multiparametric magnetic resonance imaging. Invest Radiol 53:587–595. https://doi.org/10.1097/rli.0000000000000465
49. Bickel H, Pinker-Domenig K, Bogner W, Spick C, Bago-Horvath Z, Weber M, Helbich T, Baltzer P (2015) Quantitative apparent diffusion coefficient as a noninvasive imaging biomarker for the differentiation of invasive breast cancer and ductal carcinoma in situ. Invest Radiol 50:95–100. https://doi.org/10.1097/rli.0000000000000104
50. Rahbar H, Partridge SC, Eby PR, Demartini WB, Gutierrez RL, Peacock S, Lehman CD (2011) Characterization of ductal carcinoma in situ on diffusion weighted breast MRI. Eur Radiol 21:2011–2019. https://doi.org/10.1007/s00330-011-2140-4
51. Iima M, Le Bihan D, Okumura R, Okada T, Fujimoto K, Kanao S, Tanaka S, Fujimoto M, Sakashita H, Togashi K (2011) Apparent diffusion coefficient as an MR imaging biomarker of low-risk ductal carcinoma in situ: a pilot study. Radiology 260:364–372. https://doi.org/10.1148/radiol.11101892
52. Youk JH, Son EJ, Chung J, Kim JA, Kim EK (2012) Triple-negative invasive breast cancer on dynamic contrast-enhanced

and diffusion-weighted MR imaging: comparison with other breast cancer subtypes. Eur Radiol 22:1724–1734. https://doi.org/10.1007/s00330-012-2425-2

53. Avendano D, Marino MA, Leithner D, Thakur S, Bernard-Davila B, Martinez DF, Helbich TH, Morris EA, Jochelson MS, Baltzer PAT, Clauser P, Kapetas P, Pinker K (2019) Limited role of DWI with apparent diffusion coefficient mapping in breast lesions presenting as non-mass enhancement on dynamic contrast-enhanced MRI. Breast Cancer Res 21:136. https://doi.org/10.1186/s13058-019-1208-y
54. Iima M, Partridge SC, Le Bihan D (2020) Six DWI questions you always wanted to know but were afraid to ask: clinical relevance for breast diffusion MRI. Eur Radiol. https://doi.org/10.1007/s00330-019-06648-0
55. Newitt DC, Zhang Z, Gibbs JE, Partridge SC, Chenevert TL, Rosen MA, Bolan PJ, Marques HS, Aliu S, Li W, Cimino L, Joe BN, Umphrey H, Ojeda-Fournier H, Dogan B, Oh K, Abe H, Drukteinis J, Esserman LJ, Hylton NM, ACRIN Trial Team, and I-SPY 2 TRIAL Investigators (2019) Test-retest repeatability and reproducibility of ADC measures by breast DWI: results from the ACRIN 6698 trial. J Magn Reson Imaging 49:1617–1628. https://doi.org/10.1002/jmri.26539
56. Bickelhaupt S, Paech D, Laun FB, Steudle F, Kuder TA, Mlynarska A, Bach M, Lederer W, Teiner S, Schneider S, Ladd ME, Daniel H, Stieber A, Kopp-Schneider A, Delorme S, Schlemmer HP (2017) Maximum intensity breast diffusion MRI for BI-RADS 4 lesions detected on X-ray mammography. Clin Radiol 72:900. https://doi.org/10.1016/j.crad.2017.05.017
57. Vourtsis A, Berg WA (2019) Breast density implications and supplemental screening. Eur Radiol 29:1762–1777. https://doi.org/10.1007/s00330-018-5668-8
58. Marinovich ML, Hunter KE, Macaskill P, Houssami N (2018) Breast cancer screening using tomosynthesis or mammography: a meta-analysis of cancer detection and recall. J Natl Cancer Inst 110:942–949. https://doi.org/10.1093/jnci/djy121
59. ClinicalTrials.gov (2019) Breast cancer screening with diffusion-weighted MRI in women at high risk for breast cancer. https://clinicaltrials.gov/ct2/show/NCT03835897. Accessed 16 Jan 2020